

Assessment of Corner Failure Depths in the Deep Drawing of 3D Panels Using Simplified 2D Numerical and Analytical Models

Hong Yao¹
Graduate Student

Jian Cao
Assistant Professor

Department of Mechanical Engineering,
Northwestern University,
Evanston, IL 60208

Methodologies of rapidly assessing maximum possible forming heights are needed for three-dimensional (3D) sheet metal forming processes at the preliminary design stage. In our previous work, we proposed to use an axisymmetric finite element model with an enlarged tooling and blank size to calculate the corner failure height in a 3D part forming. The amount of enlargement is called center offset, which provides a powerful means using 2D models for the prediction of 3D forming behaviors. In this work, an analytical beam model to calculate the center offset is developed. Starting from the study of a square cup forming, a simple analytical model is proposed and later generalized to problems with corners of an arbitrary geometry. The 2D axisymmetric models incorporated with calculated center offsets were compared to 3D finite element simulations for various cases. Good assessments of failure height were obtained.

[DOI: 10.1115/1.1349553]

1 Introduction

In the sheet metal forming industry, 3D finite element modeling has become a very important numerical tool to understand a specific forming process and to assist in the design of tooling and process parameters, such as binder force. However, on many occasions, a full-scale finite element simulation is considered too time-consuming to keep up with the demands of rapid design and decision making during the development of new products. It is therefore necessary to have simplified numerical models and analytical methods, which are based on the phenomenological relationships among the tooling and process parameters, to obtain a reasonable and approximate solution for the rapid design.

The methodology of using a simplified model was explored in Doege [1] where an equivalent punch diameter was found for rectangular or irregular parts by calculating a circular punch of equal cross sectional area. In other words, an axisymmetric cup with an equivalent (fictitious) diameter was used to predict the limiting draw ratio of the rectangular or irregular cup. The limiting draw ratio based on the equivalent cylinder cup was found to be lower than that of the rectangular part obtained in industrial stampings. Saran et al. [2] analyzed the forming of complex parts with irregular tooling shapes using section analysis. In each section, a plane strain condition was assumed. The analysis can successfully simulate the deformation of many local sections where the strain states are close to plane strain. Brooks et al. [3] also demonstrated the application of 2D models in the design of sheet metal forming processes. A plane strain or axisymmetric assumption was made along a critical section of the die. Since these 2D models provided quantitative and qualitative information for the die design, they helped to reduce the number of time intensive die tryouts. Walker et al. [4] suggested that axisymmetric cup analysis could provide approximate, though conservative, solutions for near axisymmetric conditions, where the circumferential stress gradient is small. Wong et al. [5], however, pointed out that a simple axisymmetric cup analysis was not adequate to mimic the

corner deep drawing of rectangular parts. If the corner part is treated as an axisymmetric cup, punch failure heights did not reach the level found in an actual 3D forming.

A novel approach to avoid conservative predictions was proposed in our previous works [6,7]. Unlike the other methods in which the axisymmetric axis is placed at O (see Fig. 1), we added a center offset to the axisymmetric model by shifting the axisymmetric axis to O' . In our work, the finite element model of a square cup (the benchmark square cup at the Numisheet'93 conference [8]) was first created as our base model. The model and its associated failure criterion using the Forming Limit Diagram were verified by physical experiments. An offset function was expressed as a function of the center strain, failure height, tooling and process parameters by fitting sample data from nearly 114 case studies of square and rectangular cups. Using this offset function, the average error of predicted forming height was reduced to 14 percent compared to 45 percent without the offset. Finally, a detailed design algorithm was provided to enable engineers to rapidly specify the right amount of the restraining force in the corner section based on the desired center strains and forming depth using the proposed 2D models.

We believe that the discrepancy in the predictions could be further reduced if the offset could be more accurately calculated. This work aims at developing an analytical model to find the center offset for corners of arbitrary geometries and to further improve the predictability of our 2D model. The analytical model is similar to a beam model. The proposed approach for assessing corner failure heights is a combination of 2D numerical simulation and analytical calculation. It uses numerical simulation, 2D axisymmetric finite element analysis, to find the failure height of the corner part whereas the 2D model adopts the center offset calculated from the beam model. We verified our predictions with full-scale 3D FEM simulations.

The layout of this paper is as follows. Definitions of tooling geometric parameters are defined in Section 2 to provide a clear overview of the parameters involved. Section 3 derived the simple analytical formulation for calculating the offsets for the base model shown in Fig. 5. Constants in the analytical model were determined by fitting the results to those obtained from 3D finite element simulations of the base model. These constants are not expected to change in the following generalization process. Sec-

¹Dr. Hong Yao is now working at National Steel Corporation, Livonia, Michigan.

Contributed by the Manufacturing Engineering Division for publication in the JOURNAL OF MANUFACTURING SCIENCE AND ENGINEERING. Manuscript received Sept. 1999; revised April 2000. Associate Editor: K. Stelson.

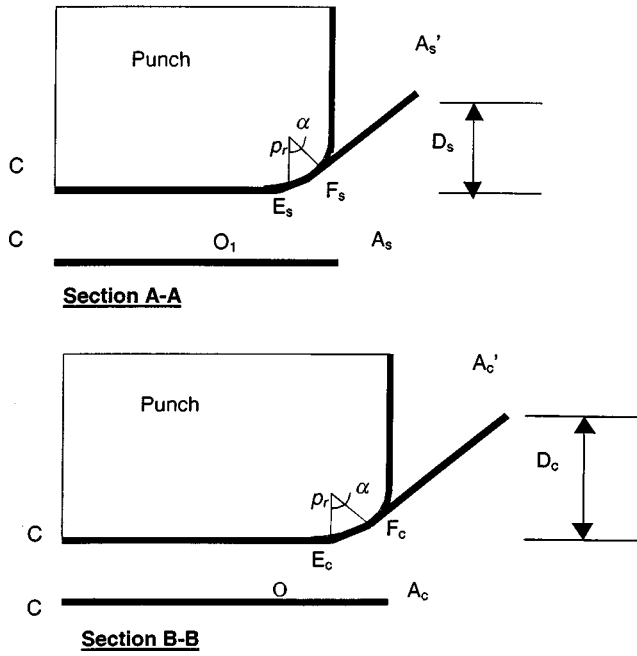


Fig. 4 Illustrations of the side and corner stretch heights

$$B = \frac{1}{2}(B_1 + B_2) \quad (2)$$

and k is the draw ratio factor reflecting the draw ratio change compared to that of the base model, i.e.,

$$k = \frac{d_1 d_2}{d_0 d} \quad (3)$$

where $d_0 = (B_0 - c_0)/P_0$ (punch size $P_0 = 35$ mm), $d_1 = (B_1 - c)/P_1$, $d_2 = (B_2 - c)/P_2$ and d is the averaged draw ratio defined by

$$d = \frac{1}{2}(d_1 + d_2) \quad (4)$$

Using the concept of the size of the model, below are the definitions for the normalized punch size, \hat{P} , punch nose radius, \hat{p}_r , and punch plan view radius, \hat{R}_p , which are

$$\hat{P} = \frac{(P_1 + P_2)}{2SP_0} \quad (5)$$

$$\hat{p}_r = \frac{p_r}{Sp_{r0}} \quad (6)$$

$$\hat{R}_p = \frac{R_p}{SR_{p0}} \quad (7)$$

where the punch nose radius p_{r0} and the plan view radius R_{p0} in the base model are 8 mm and 10 mm, respectively.

2.2 2D Model with a Center Offset. Our previous works [6,7] introduced a simplified 2D axisymmetric model for predicting the tearing failure height in a corner section of a complicated 3D part. Figure 1 shows the plan view of a quarter of a rectangular cup and slices of simplified axisymmetric models. The conventional method treats the corner part (OFGH) as an axisymmetric cup and use OMN as the simplified 2D axisymmetric model. As a result the model does not take into account the material stretched into the corner section from under the punch and the material flowing toward the corner from the straight sides as the punch advances. Moreover, such a model cannot reflect the effects

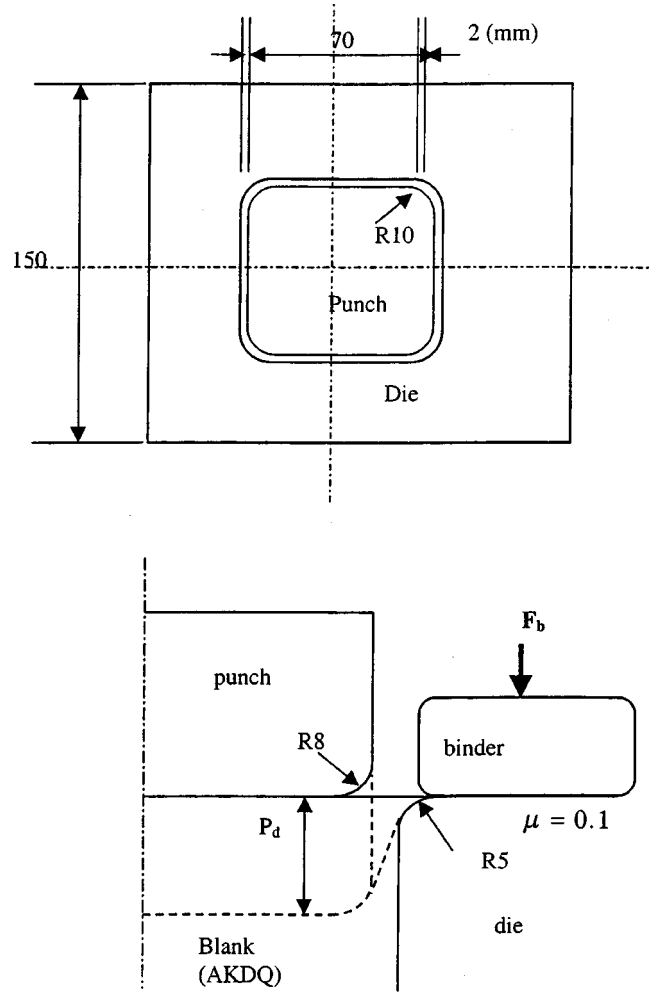


Fig. 5 Illustration of the geometry and process of the base model

caused by varying the size and aspect ratios of the punch. Consequently, it provides conservative results, meaning that the corners can actually be formed deeper than that predicted. Figure 1 also shows our proposed axisymmetric model, $O'M'N'$, with a center offset r_{off} . The deformation of the extra material under the punch brought about by the offset will delay the failure of the axisymmetric part. As a result, the 2D model with an adequate offset can reach the failure height of the 3D model and can be used to design the appropriate restraining force for the desired forming operation. Notice that, here, "failure" is referring to tearing failure. Another important failure mode, wrinkling, has been studied in Cao and Wang [9] and Wang and Cao [10].

2.3 Stretch Heights. In Section A-A and Section B-B of Fig. 4, D_s and D_c represent the side and corner stretch heights, respectively. Assuming the sheet metal section CA_s is formed upon the punch at the contact angle α as in Section A-A, the tangential point at which the blank separates the punch nose is point F_s . Now let the length CA_s in the undeformed configuration be equal to the length of CE_sF_s . The material point A_s will be deformed to point A'_s . The distance measured vertically from the bottom of the punch to A'_s is defined as the side stretch height, D_s . Similarly, the corner stretch height, D_c , can be defined. The corner and side stretch heights indicate how much material is pulled out from underneath the punch and they are directly related to the final forming height.

Simulation results demonstrated that the corner stretch height

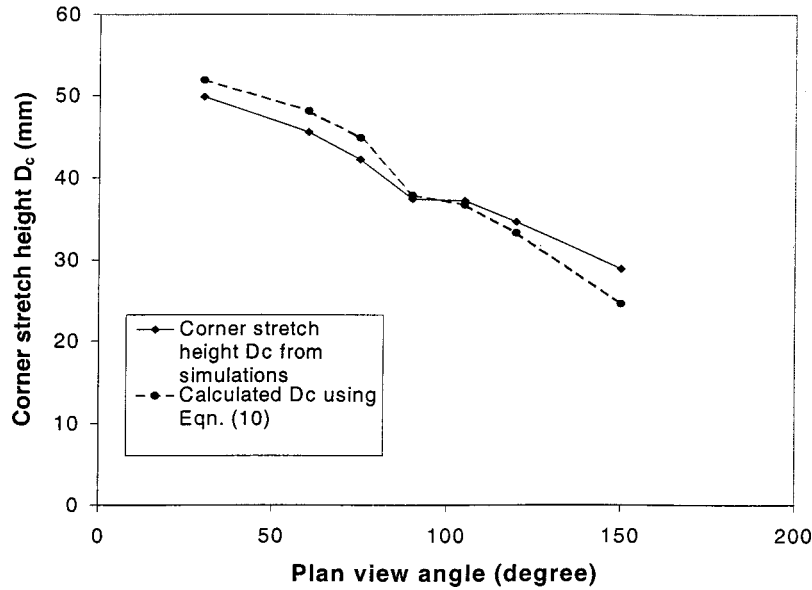


Fig. 6 Comparison of the calculated corner stretch heights to the simulation results

D_c is always larger than the side stretch height D_s . For square cups, D_c is approximately the vector sum of D_s , i.e.,

$$D_c^2 = D_s^2 + D_s^2 \quad (8)$$

Therefore the difference of D_c and D_s can be approximated as:

$$D_c - D_s = (\sqrt{2} - 1)D_s \approx 0.4D_s \quad (9)$$

Equation (9) is then generalized for rectangular and nonrectangular cups, i.e., by using D_s and plan view angle θ .

$$D_c - D_s = 0.4\sqrt{1 - \cos \theta}D_s \quad (10)$$

where D_s is the average of the side stretch heights, D_{s1} and D_{s2} , at the plane strain sections ($D_s = (D_{s1} + D_{s2})/2$). Figure 6 shows the comparison of the calculated corner stretch heights to the 3D FEM simulation results for cases, which are about five times larger than the base model and have plan view angles varied from 30 to 150 deg. Very good approximations are obtained.

3 Finding the Offset for the Base Model

The right offset is obtained when the failure height predicted by the 2D model (y_p^{2d}) matches that in the 3D model (P_d). Obviously, offset depends on the specific tooling geometry and process parameters such as material properties and binder force, etc. To deal with this complicated problem, an analytical model will first be developed to calculate the offset for the base model in this section and will be generalized to the arbitrary corner geometry in Section 4.

As mentioned in Section 2.3, stretch height is directly related to the final failure height. Our approach is to relate the stretch height difference at the corner and straight sides of the 3D model, to a simplified analytical model, which can be used to calculate the offset. As illustrated in Fig. 4, stretch height difference, Δ , which is the difference of the displacements between A'_c and A'_s due to the material stretching at sections OA_c and O_1A_s (Figs. 1–4), can be calculated as:

$$\Delta = D_c - D_s = \frac{0.4D_s}{\sin \alpha} - 0.4\varepsilon_c(P_0 - R_{p0}) \quad (11)$$

where α is the contact angle, a constant 0.4 comes from Eq. (9) and ε_c is the averaged principal strain at the center of the blank (point C in Figs. 1–3). Since the offset is an additional material

amount added to consider the material stretching underneath the punch, we related the offset to the averaged principal strain at the center of the pan. The center strain is considered as an important design specification in the stamping part, as this value relates directly to the strength of the panel. When designing the plane strain section, the 2D section analysis model can be used to find the center strain under certain restraining forces or start from the center strain to find the restraining force. The second term in Eq. (11) reflects the difference of the displacements caused by the material stretch at sections CO and CO₁ underneath the punch.

The difference of the stretch heights ($D_c - D_s$) is partially caused by the fact that the restraining force applied at the corner and the straight sides are different. If the total binder force applied at the quarter of the box is F_b , the binder force per unit length along the binder inner profile at the straight side (Fig. 2), F_s , and at the corner part, F_c , can be expressed as:

$$F_s = \frac{A_1 F_b}{(A_1 + A_2 + A_3)(P_1 - R_p) \tan \beta_1} \quad (12)$$

$$F_c = \frac{A_3 F_b}{(A_1 + A_2 + A_3)(R_p + c + d_r) \theta} \quad (13)$$

where A_1 (KHJ) and A_2 (DEFL) are contact areas at the straight sides, A_3 (FGHKL in Figs. 1 and 2 and FGG'HKL in Fig. 3) is the binder contact area at the corner, and as illustrated in Figs. 1–3, $\theta = \beta_1 + \beta_2$.

The difference of the restraining stress, σ , at the draw wall area can therefore be defined as

$$\sigma = \frac{2\mu(F_c - F_s)e^{\mu\alpha}}{t} \quad (14)$$

where t is the thickness of the blank, α is the contact angle as shown in Fig. 4 and μ is the friction coefficient.

Figure 7 illustrates the schematic of our analytical model used to calculate the center offset. The arc is subjected to a uniform distributed load, which is equal to the difference of restraining stress, σ . The angle $\theta/2$ is half of the plan view angle. As illustrated in Fig. 7 and section B-B of Fig. 4, the radius of the middle surface of the arc consists of three quantities. They are half of the

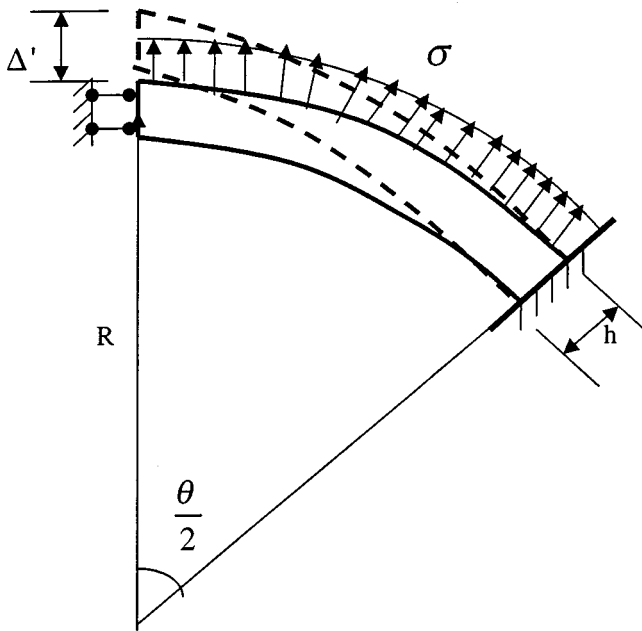


Fig. 7 Simplified analytical model for calculating the offset

arc beam height (h), the horizontal distance from the center of the corner point O to the tangential point F_c , and a quantity related to the offset of the 2D model. Therefore,

$$R = (R_{p0} - p_{r0}(1 - \sin \alpha)) + \hat{r}_{off} + h/2 \quad (15)$$

where h is the length of $F_s A'_s$, i.e.

$$h = \frac{(D_s - p_{r0}(1 - \cos \alpha))}{\sin \alpha} \quad (16)$$

and \hat{r}_{off} is found to be a variable related to the center average principal strain and the offset. Using numerical simulation results of the base model, we found that the offset is inversely proportional to the center strain, when the center strain is larger than 4 percent. For the base model, this relation can be approximated as:

$$\hat{r}_{off} = r_{off}(a_1 \varepsilon_c + a_2)^n \quad (17)$$

where a_1 , a_2 and n are fitting parameters obtained using 3D FEM simulations and have the values of 6.5, 0.63 and 1.5, respectively.

Assume the deformation is elastic, the solution of the deflection can be approximated as

$$\Delta' = \gamma \frac{\sigma R^2}{Eh} \left(\frac{t_0}{t} \right) \quad (18)$$

where E is the Young's modulus of the material, t is the thickness in mm and t_0 is 1 (mm), and γ is a constant. Equation (18) is then used to relate the offset to the wall stretch height difference, Δ , for the base model. When $\gamma=1$, the offset that will match the failure heights of 2D and 3D models can be found by

$$\Delta = \Delta' \quad (19)$$

Notice that the value of γ used here is not the one in the exact solution of the elastic deflection of the curved beam under a distributed load σ . In our formulation, γ is adjustable according to material properties. The recommended value for γ is 1.0 for steel and 0.9 for aluminum.

Using Eqs. (14)–(19) the offset in the 2D axisymmetric model can be calculated by

$$r_{off} = \left[\left(\frac{Eht}{\gamma t_0 \sigma} \Delta \right)^{1/2} - \frac{h}{2} - R_{p0} + p_{r0}(1 - \sin \alpha) \right] \frac{1}{(a_1 \varepsilon_c + a_2)^n} \quad (20)$$

The failure depths obtained from 2D axisymmetric models using the calculated offsets are plotted versus the center strain and compared with the 3D FEM simulation and experimental results as shown in Fig. 8. For the cases when center strains are larger than 4 percent, the averaged error of failure height predictions is only 6.9 percent. Notice that the center strain of 5 percent is desired in most industrial applications to ensure the stiffness of the formed sheet panel. Figure 8 demonstrates that our analytical beam model provides reasonable estimations of center offsets, which lead to good assessments of failure heights using modified 2D axisymmetric models.

4 Generalization of the Offset Function

The effectiveness of the analytical model for the base model demonstrated in the last section indicates that our formulation has reflected the phenomenological relationships among the key process parameters. Generalization of the formulation with respect to

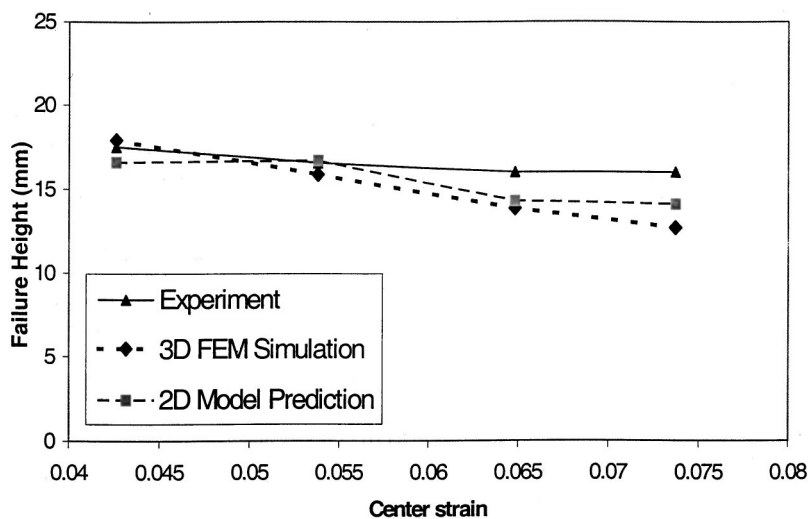


Fig. 8 Comparison of failure heights predicted by using the analytical model to simulate results for the base model

Table 1 *Geometry of square cup with geometry, friction and material variation

Case No.	Material	FLD ₀	μ	P ₁ X _P ₂ (mm)	B ₁ X _B ₂ (mm)	c (mm)
AKDQ_f10_s1cl1	AKDQ	0.3	0.10	35x35	75x75	2
AKDQ_f10_s5cl1	AKDQ	0.3	0.10	175x175	375x375	10
AKDQ_f10_s10cl1	AKDQ	0.3	0.10	350x350	750x750	20
AKDQ_f10_s5cl5	AKDQ	0.3	0.10	175x175	415x415	50
AKDQ_f10_s5cl10	AKDQ	0.3	0.10	175x175	415x415	50
AKDQ_f15_s5cl5	AKDQ	0.3	0.15	175x175	415x415	50
AKDQ_f06_s5cl5	AKDQ	0.3	0.06	175x175	415x415	50
A180DR_f10_s5cl5	A180DR	0.3	0.10	175x175	415x415	50
AA6111_f10_s5cl5	AA6111	0.223	0.10	175x175	415x415	50

- * 1.The geometry of case AKDQ_f10_s1cl1 is the square cup of Base model.
- 2.All geometric parameters are illustrated in Figs. 1-3.
- 3.The thickness of the blank is kept at 0.796 mm in all the models of steel and 1.0 mm for models of Aluminum.
- 4. Material types:
 180DR ---- High strength steel
 AA6111 ---- Aluminum AL6111-T4
 AKQD ---- Mild steel used in our experiment

those parameters can finally yield an analytical formulation for a general process. This section shows how the formulation will be generalized.

In the formulation for the base model, the offset was determined by matching the failure heights of the 2D and 3D models. For the general cases, the offset determination should consider the variations of the draw ratio, k , and plan view angle, θ , compared to the base model. Therefore, as a design tool, the failure heights reached by the 2D model, y_p^{2d} , should be equal to the normalized 3D failure height, \hat{P}_d , i.e.,

$$y_p^{2d} = \hat{P}_d = f(k, \theta, P_d) \quad (21)$$

Since the actual failure height P_d increases as the plan view angle decreases and the draw ratio factor, the normalized failure height, \hat{P}_d , is defined as:

$$\hat{P}_d = k P_d \sqrt{1 - \frac{1}{2} \cos \theta} \quad (22)$$

As the averaged principal strain at the center of the blank is sensitive to the friction coefficient and the punch size, the normalized center strain is expressed as

$$\hat{\epsilon}_c = \epsilon_c(\hat{P})^{3.5} \left(\frac{\mu}{\mu_0} \right) \quad (23)$$

where $\mu_0 = 0.1$, \hat{P} is the normalized punch size defined by Eq. (5). The significance of this normalization is to keep the relationship between the offset and the center strain remaining the same as formulated by Eq. (17). Also considering the effects of the size of the model, S , which is defined in Eq. (1), and the forming limit of the sheet metal, FLD₀, under the plane strain loading path, the general relation between the center strain and offset is updated to be

$$\hat{r}_{off} = r_{off} H(a_1 \hat{\epsilon}_c + a_2)^n \quad (24)$$

where H is formed as

$$H = 1 + (\sqrt{S} - 1)(0.3/FLD_0 - 1) \quad (25)$$

The \hat{r}_{off} in Eq. (25) will be obtained the same way as it was for the base model but using the updated equations formulated with normalized parameters as defined above.

The generalized quantity, which represents the difference of displacements between A'_c and A'_s , can be expressed as:

$$\hat{\Delta} = \frac{0.4(1 - \cos \theta)^{1/2} k^{1/2} \left[\frac{\hat{D}_s}{\sin \alpha} - \frac{\epsilon_c(P - R_p)}{S} \right]}{\hat{R}_p^{1/2} \hat{p}_r^{3/2}} \quad (26)$$

where k is the draw ratio factor defined in Eq. (3), \hat{R}_p and \hat{p}_r are normalized punch nose and plan view radii, respectively, defined in Eqs. (6) and (7), and \hat{D}_s is the generalized stretch height in consideration of the size of the model, plan view angle and the forming limit of the sheet metal, i.e.,

$$\hat{D}_s = D_s [H + (\sqrt{S} - 1)(1 - \sin \theta)] \quad (27)$$

The radius of the arc is proportional to the size of the model, i.e.,

$$\hat{R} = S [R_p + \hat{r}_{off} - p_r(1 - \sin \alpha)] + \hat{h}/2 \quad (28)$$

The height of the curved beam is also proportional to the size of the model, i.e.,

$$\hat{h} = \frac{S(\hat{D}_s - p_r(1 - \cos \alpha))}{\sin \alpha} \quad (29)$$

Using Eqs. (14), (18) and (23)–(29), the offset for a 3D model can be calculated as

$$r_{off} = \left\{ \left[\left(\frac{E \hat{h} t}{\gamma t_0 \sigma} \hat{\Delta} \right)^{1/2} - \frac{\hat{h}}{2} \right] \frac{1}{S} - R_p + p_r(1 - \sin \alpha) \right\} \frac{1}{H(a_1 \hat{\epsilon}_c + a_2)^n} \quad (30)$$

In the generalization process illustrated above, many geometric and process parameters are normalized using geometric parameters. Several exponent constants in Eqs. (23) and (26) are decided using the real offsets obtained through the 2D and 3D simulation results of Tables 1 to 3. Due to the fact that we have examined a wide range of part geometry, friction condition and process parameters, these constants are expected to reflect the implicit phenomenological relationship between the center offset and all the above factors. Further examination of the accuracy of failure height prediction for cases not used in the fitting process will be presented in the following section.

5 Accuracy Assessment of Failure Height Prediction and Design Algorithm

3D FEM simulation is used to test the failure height predictability of the proposed axisymmetric model with the center offset

Table 2 Geometric parameters of square and rectangular cups with draw ratio and aspect ratio variation

Case Number	Material	FLD ₀	μ	P ₁ X _P ₂ (mm)	B ₁ X _B ₂ (mm)	c (mm)
S1cl5_1_1_1	AKDQ	0.3	0.10	60 X 60	108x108	10
S1cl1_0.5_1_1	AKDQ	0.3	0.10	60X 35	100x75	2
S1cl1_0.5_1_1.5	AKDQ	0.3	0.10	85 X 35	125x75	2
S1cl5_1_1_2	AKDQ	0.3	0.10	110 X 60	158x108	10
S5cl5_1_1_1	AKDQ	0.3	0.10	300 X 300	540x540	50
S5cl5_1_1_2	AKDQ	0.3	0.10	550X300	790x665	50
S5cl1_0.5_1_1	AKDQ	0.3	0.10	300X175	500x375	10
S1cl5_2_1_3	AKDQ	0.3	0.10	160 X 110	208x158	10

calculated from our analytical beam model and to detect the limitations of the approach. The predictability of Eq. (30) was first verified using the square and rectangular box forming simulations. The examined cases include variations in the punch size, the die clearance, plan view radius, punch nose radius etc. as given in Tables 1–3. For each case, various binder forces, ranging from one that barely caused the cup to split to one beyond which the failure height levels off, were applied in the simulations. Friction coefficients of 0.06, 0.1 and 0.15 and different materials of steel and aluminum were also used. The geometric and process parameters used in these cases are given in Tables 1–3. Figure 9 shows the comparison of the error of the failure height prediction using the empirical offset function² [7] and using our analytical model, Eq. (30). The averaged error of failure height predictions of this new approach is reduced to 13 percent compared to 45.6 percent when no offset was used and 14 percent when the empirical offset function was used. The chance to have the error below 10 percent is increased to 49 percent, compared to 44 percent when the empirical offset function was used. Only in a few cases were the errors above 30 percent. These were the cases when the cup barely reached failure under a low binder force. In these cases, a small inaccuracy of the predicted offset can lead to a false non-failure result. Therefore, special care needs to be taken when low binder forces are used to reach deep forming heights with small center strains.

The analytical model has been further used to predict the corner failure depth of panels of different sizes with plan view angles varying from 30 to 150 deg (Table 4). Table 5 lists the failure heights calculated from 3D FEM analysis, 2D axisymmetric analysis with and without center offset, and calculated center offset using Eq. (30). Notice that these cases were not used in any means in the process of developing our analytical model. The averaged error of failure height predictions with offsets is only 11.8 percent compared to 42.3 percent without offsets.

The proposed analytical offset function (Eq. (30)) can be used in designing the corner part of 3D panels. For a given combination of material, geometric and strength requirements, tooling and process parameters, such as restraining force, lubrication, blank size and tooling, can be varied and finalized using the 2D axisymmetric model with a center offset. A detailed flow chart of this design process using simplified analytical and numerical models is given in Fig. 10. Finally, the model may need to be used in conjunction with other 2D models. For example, 2D section analysis may be needed in the plane strain section to calculate the side stretch height, D_s before the offset can be solved.

²The empirical offset function proposed by the authors [7] was:

$$r_{off} = \left(\frac{\hat{R}_p^{0.5}}{\hat{p}_r^{0.7}} \right) \frac{0.358FLD_0^{2.1286} k^{1.3853}}{e^{1.4106} p^{4.2318} \gamma_p^{0.4334} C_p^{0.6411} \mu^{1.0643}}$$

where \hat{R}_p and \hat{p}_r are the same as defined in this work and the other parameters were defined in our previous work [7].

6 Conclusions

An analytical model has been formulated to calculate the offsets of the simplified 2D axisymmetric models for predicting the failure height of 3D parts. The effectiveness of the formulation for the base model, a Numisheet'93 square cup forming (Fig. 5), proves its conformity to the phenomenological relationship between the process parameters and required center offset of the 2D model. A generalization of the formulation with normalized process parameters finally extends its ability to calculate offsets for the design of general forming processes. Using the proposed analytical model, the offset has been successfully calculated not only for rectangular panels (Fig. 9) but also for panels with plan view angle variations (Table 5). The accuracy of the failure height prediction using the 2D model with offset has been improved. It also

Table 3 Geometric parameters for square cups with different tooling corner radii

Case	P ₁ X _P ₂ (mm)	B ₁ X _B ₂ (mm)	c (mm)	p _r (mm)	R _p
R20p10	135X135	415X415	50	10	20
R50p10	135X135	415X415	50	10	50
R100p10	135X135	415X415	50	10	100
R20p20	135X135	415X415	50	20	20
R30p20	135X135	415X415	50	20	30
R40p20	135X135	415X415	50	20	40
R50p20	135X135	415X415	50	20	50
R60p20	135X135	415X415	50	20	60
R70p20	135X135	415X415	50	20	70
R80p20	135X135	415X415	50	20	80
R100p20	135X135	415X415	50	20	100
R125p20	135X135	415X415	50	20	125
R150p20	135X135	415X415	50	20	150
R40p40	135X135	415X415	50	40	40
R50p40	135X135	415X415	50	40	50
R60p40	135X135	415X415	50	40	60
R80p40	135X135	415X415	50	40	80
R100p40	135X135	415X415	50	40	100
R125p40	135X135	415X415	50	40	125

Note: Binder force = 60KN, die radius =25 mm.

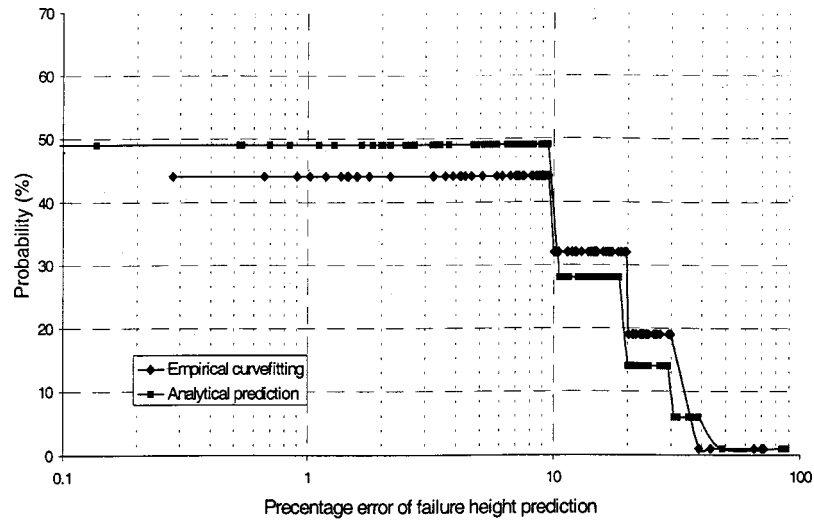


Fig. 9 Comparison of the probability of errors in the failure height prediction

Table 4 Geometry parameters for panels with geometry and plan view angle variation

Models	F_b (N)	P_1 (mm)	P_2 (mm)	R_p (mm)	p_r (mm)	d_r (mm)	c (mm)	B (mm)	θ ($^\circ$)
s5cl5_30	400000	516.5	516.5	50	40	25	50	165	30
s5cl5_60	300000	266.5	266.5	50	40	25	50	165	60
S5cl5_75	300000	212.9	212.9	50	40	25	50	165	75
S5cl5_90	300000	175	175	50	40	25	50	165	90
S5cl5_105	300000	145.9	145.9	50	40	25	50	165	105
S5cl5_120	300000	122.2	122.2	50	40	25	50	165	120
S5cl5_150	300000	83.49	83.49	50	40	25	50	165	150
S1cl5_112_75	128884	126.9	88.56	10	8	5	10	33	75
S1cl5_112_90	128884	110	60	10	8	5	10	33	90
S1cl5_112_105	128884	100.1	34.97	10	8	5	10	33	105

Table 5 Failure height predictions of cases in Table 4 using 2D axisymmetric models with and without offsets

Models	Binder Force F_b (N)	Failure Height P_d (mm) (3D FEM)	Calculated Offset (mm)	With Offset		Without Offset	
				P_d (mm)	Error	P_d (mm)	Error
S5cl5_30	400000	106.3	14.45	127.6	20%	120.5	13%
S5cl5_60	300000	128.6	57.38	107.6	-16%	83.7	-35%
S5cl5_75	300000	118.2	86.16	106.7	-10%	70.3	-41%
S5cl5_90	300000	104.7	117.16	98.4	-6%	59.5	-43%
S5cl5_105	300000	103.0	173.63	88.1	-14%	50.7	-51%
S5cl5_120	300000	98.8	266.62	81.7	-17%	43.4	-56%
S5cl5_150	300000	86.2	604.30	100.0	16%	31.6	-63%
S1cl5_112_75	128884	28.7	21.02	29.7	4%	16.4	-41%
S1cl5_112_90	128884	22.96	25.00	26.2	14%	14.1	-34%
S1cl5_112_105	128884	21.619	20.59	21.5	-0.5%	11.8	-46%
Averaged absolute error					11.8%		42.3%

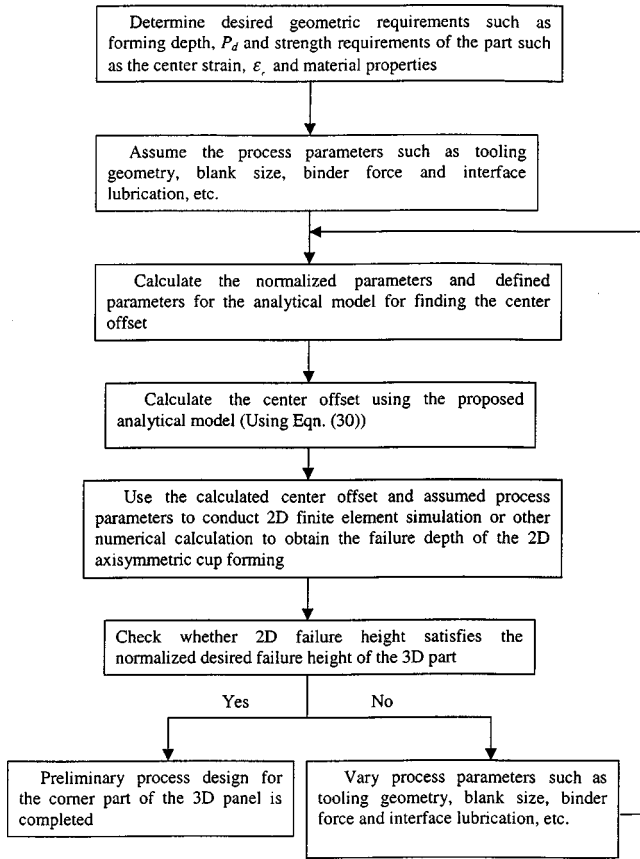


Fig. 10 Flow chart of the process parameter design using simplified analytical and numerical models

needs to be mentioned here that the failure height prediction should be used in the preliminary design stage, which requires the failure depth prediction having a reasonable accuracy for decision making at that stage. Such predictions are not intended for the final design stage, where a full-scale 3D FEM simulation might be more desired.

In the proposed formulation for finding the offset, some constants and exponents are used such that the offset calculated from the formulation can be reasonably accurate to match the failure height results obtained from the experiments or 3D FEM simulations. However, these numbers are not expected to vary from case to case. In the generalization of the model to arbitrary cases, many geometric and process parameters are normalized using geometric parameters. Therefore, unlike the authors previous paper [6,7], which obtained the offset function through empirical fits, the offset function proposed in this paper involves some empirical parameters but basically is formulated and derived using the analytical models.

Some specific limitations of our 2D models are worthy of our attention. As mentioned before, in the case when low binder forces are used to reach deep forming heights with low center strains, 2D models with an estimated offset may fail to predict the failure. Care also needs to be taken when determining the geometry of the corner model, which is based on the locations of the plane strain sections. For a complicated part, locating the plane strain sections correctly is important to the effectiveness of the design using 2D models.

Acknowledgments

The authors would like to express appreciation to General Motors and the National Science Foundation for their financial support.

Nomenclature

Geometric Parameters (Illustrated in Figs. 1–4)

- B_1, B_2 = blank size measured from the center of the blank
- P_1, P_2 = punch size measured from the center of the blank
- c = punch die clearance
- R_p = plan view radius
- θ = plan view angle
- β_1, β_2 = plan view angles measured from the plane strain section
- d_r = die corner radius
- b = blank clamped between binder and die
- p_r = punch radius
- α = contact angle
- B_0 = half of the blank size of the base model, $B_0 = 75$ mm
- c_0 = punch die clearance of the base model, $c_0 = 2$ mm
- P_0 = punch size measured from the center of the blank, $P_0 = 35$ mm
- p_{r0} = punch radius of the base model, $p_{r0} = 8$ mm
- R_{p0} = plan view radius of the base model, $R_{p0} = 10$ mm
- A_1, A_2 = contact areas at the straight sections of the die
- A_3 = total contact area
- t = thickness of the sheet metal
- t_0 = thickness of 1 mm

Process Parameters

- F_b = total binder force
- F_s = side restraining force per unit length
- F_c = corner restraining force per unit length
- μ = interface friction coefficient
- μ_0 = interface friction coefficient of 0.1
- ε_c = center averaged principal strain
- y_p^{2d} = failure height of the 2D model
- P_d = failure height of the 3D model
- E = Young's modulus
- FLD_0 = forming limit of the sheet metal under plane strain loading path

Normalized Parameters

- \hat{P} = normalized punch size
- \hat{p}_r = normalized punch corner radius
- \hat{R}_p = normalized plan view radius
- \hat{r}_{off} = normalized Offset
- \hat{P}_d = normalized forming failure height
- $\hat{\varepsilon}_c$ = normalized center strain
- \hat{D}_s = normalized side stretch height
- \hat{R} = normalized radius of the analytical arc beam
- \hat{h} = normalized height of the analytical arc beam
- $\hat{\Delta}$ = normalized wall stretching difference

Defined Parameters for the Formulation

- r_{off} = center offset
- S = size of the model
- k = draw ratio factor
- B = averaged blank size
- d = averaged draw ratio factor
- d_1 = draw ratio in direction of the 1st plane strain section
- d_2 = draw ratio in direction of the 2nd plane strain section
- d_0 = draw ratio of the base model
- D_c = corner stretch height
- D_s = averaged side stretch height
- D_{s1} = side stretch height along the 1st plane strain section
- D_{s2} = side stretch height along the 2nd plane strain section
- Δ = wall stretching difference
- σ = difference of restraining stress
- H = offset modification parameter
- R = radius of the analytical arc beam
- h = height of the analytical arc beam

Δ' = approximate elastic deflection of the arc beam

Fitting Parameters

- $a_1 = 6.5$ (obtained from the base model)
- $a_2 = 0.63$ (obtained from the base model)
- $n = 1.5$ (obtained from the base model)
- $\gamma = 1$ for steel and 0.9 for aluminum

References

- [1] Doege, E., 1985, "Prediction of Failure in Deep Drawing," *Proceedings of the 12th Automotive Materials Symposium*.
- [2] Saran, M. J., Keum, Y. T., and Wagoner, R. H., 1991, "Section Analysis with Irregular Tools and Arbitrary Draw-in Conditions for Numerical Simulation of Sheet Forming," *Int. J. Mech. Sci.*, **33**, No. 11, pp. 893–909.
- [3] Brooks, A., Jhita, R., and Ni, C. M., 1991, "Applications of a Two-Dimensional Metal Forming Analysis Tool to Production Stamping Problems," *SAE Trans.*, **100**, Sect 5, pp. 751–758.
- [4] Walker, T., Kolodziejcki, J., and Karima, M., 1992, "Using Axisymmetric Solutions to Estimate the Forming Severity of Three Dimensional Metal Stampings," *SAE Paper 920636, Autobody Stamping Applications and Analysis, SAE SP-897*, pp. 161–172.
- [5] Wong, C., Wagoner, R. H., and Wenner, M. L., 1997, "Corner Design in Deep Drawn Rectangular Parts," *SAE Paper 970437*, pp. 39–55.
- [6] Yao, H., Kinsey, B., and Cao, J., 1999, "A Simplified 2D Model in Predicting Failure in a Square Part," *SAE Technical Paper Series 1999-01-1317*.
- [7] Yao, H., Kinsey, B., and Cao, J., 2000, "Rapid Design of Corner Restraining Force in Deep Drawn Rectangular Parts," *Int. J. Mach. Tools Manuf.*, **40**, pp. 113–131.
- [8] Makinouchi, A., Nakamachi, E., Onate, E., and Wagoner, R. H., 1993, "Numerical Simulation of 3-D Sheet Metal Forming Processes Verification of Simulation with Experiment," *Proceedings of the 2nd International Conference Numisheet'93*.
- [9] Cao, J., and Wang, X., 1999, "An Analytical Model for Plate Wrinkling Under Tri-Axial Loading and Its Application," *Int. J. Mech. Sci.*, **42**, No. 3, pp. 617–633.
- [10] Wang, X., and Cao, J., 2000, "On the Prediction of Side-Wall Wrinkling in Sheet Metal Forming Process," *Int. J. Mech. Sci.*, **42**, No. 12, pp. 1105–1129.